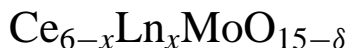


Study on structure and oxide ionic conductivity for new compound



Ping Che^a, Qibing Bo^b, Jing Feng^a, Qiuyan Wang^c, Xueqiang Cao^a, Jian Meng^{a,*}

^a Key Laboratory of Rare Earth Chemistry and Physics, Changchun Institute of Applied Chemistry, Chinese Academy of Sciences, Changchun 130022, PR China

^b College of Chemistry and Chemical Engineering, Jinan University, Shandong Jinan 250000, PR China

^c Changchun College of Chinese Medicine, Jilin Changchun 130000, China

Received 30 July 2004; received in revised form 1 December 2004; accepted 15 December 2004

Available online 2 June 2005

Abstract

A new compound $\text{Ce}_{6-x}\text{Ln}_x\text{MoO}_{15-\delta}$ has been synthesized by wet-chemistry method. Their crystal structure and oxide ionic conductivity were characterized by powder X-ray diffraction, Raman, IR spectrum and A.C. impedance technique. The XRD results showed that $\text{Ce}_6\text{MoO}_{15-\delta}$, $\text{Ce}_5\text{LnMoO}_{15-\delta}$ have cubic symmetry with $Fm\bar{3}m$ space group. The refined lattice parameters showed that their lattice constants decrease with the decrease of the ionic radius of Ln^{3+} . The electrochemical measurements showed that the ionic conductivity of resulting oxides $\text{Ce}_{6-x}\text{Ln}_x\text{MoO}_{15-\delta}$ have an enhance, which may be a kind of promising material for SOFCs.

© 2005 Elsevier B.V. All rights reserved.

Keywords: Solid state electrolyte; $\text{Ce}_{6-x}\text{Ln}_x\text{MoO}_{15-\delta}$; Ionic conductivity; SOFCs

1. Introduction

Oxide ion conductors are important functional materials, which can be used as electrolytes for fuel cells, oxygen sensors and films for separating oxygen from air. The most successful solid state oxide electrolytes have been developed on one of the oxides ZrO_2 [1], HfO_2 , ThO_2 , Bi_2O_3 [2] or CeO_2 [3], LaGaO_3 [4–6] $\text{La}_2\text{Mo}_2\text{O}_9$ [7], and La_2GeO_5 [8]. We report here the preparation and characterization of new compound $\text{Ce}_6\text{MoO}_{15-\delta}$ as well as the substitution of Ln (Ln = Y, Pr, Sm, Gd, Tb, Dy, Ho, Er and Yb) for Ce, which all exhibit good oxide ionic conductivity.

2. Experimental

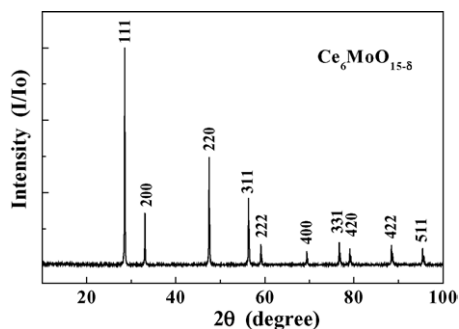
$\text{Ce}_6\text{MoO}_{15-\delta}$, $\text{Ce}_5\text{LnMoO}_{15-\delta}$ and $\text{Ce}_{5/6}\text{Y}_{1/6}\text{O}_{2-\delta}$ compounds were prepared by using a modified citrate complexa-

tion method and fired in 900 °C for 20 h [9]. The starting salts are rare-earth nitrate hexahydrated ($\text{Ln}(\text{NO}_3)_3 \cdot 6\text{H}_2\text{O}$ (purity of 99.99%)), hexammonium heptamolybdate hexahydrated ($(\text{NH}_4)_6\text{Mo}_7\text{O}_{24} \cdot 6\text{H}_2\text{O}$ (purity of 99.99%)) and citric acid with purity of 99.99%. The X-ray diffraction (XRD) patterns were recorded on a Rigaku D/max-IIB X-ray diffractometer. Their crystal structure was analyzed using the CELL refinement software written by Takaki et al. [10]. Oxide ionic conductivity was measured by A.C. impedance technique with a frequency response analyzer (Solatron 1255 + 1287) on the sintered disk (\varnothing 12 mm and 2 mm in thickness) with Pt electrode deposited on both surfaces. Curve fitting and conductivity calculation were done by using Zview software. XPS were measured on an EXCA-LAS MK II X-ray photoelectron spectrometer from VG Co.

3. Results and discussion

Fig. 1 shows a typical X-ray powder diffraction patterns of $\text{Ce}_6\text{MoO}_{15-\delta}$. From Fig. 1, it is obvious that $\text{Ce}_6\text{MoO}_{15-\delta}$,

* Corresponding author. Tel.: +86 431 5262030; fax: +86 431 5698041.
E-mail address: jmeng@ciac.jl.cn (J. Meng).

Fig. 1. XRD of $\text{Ce}_6\text{MoO}_{15-\delta}$.

Ln-doping samples $\text{Ce}_5\text{LnMoO}_{15-\delta}$ and $\text{Ce}_{5/6}\text{Y}_{1/6}\text{O}_{2-\delta}$ have the same of diffraction patterns. It suggests that the new solid solutions have the same structure with fluorite-related compounds CeO_2 (JCPDS 43-1002). Through the analysis of lattice constant, we can see that the shifts of lattice parameter are directly correlated with the decrease in ionic size of rare earths. This result is fairly in agreement with that of $\text{Ce}_{1-x}\text{Ln}_x\text{O}_{2-\delta}$ ($\text{Ln} = \text{La}, \text{Pr}, \text{Nd}, \text{Eu}, \text{Gd}$ and Tb) [11].

To investigate the valence states of Ce and Mo ions in the solid solution $\text{Ce}_6\text{MoO}_{15-\delta}$, XPS were measured at room temperature, using the standard CeO_2 as reference. The core level spectra of Ce 3d and Mo 3d are shown in Fig. 2. From Fig. 2, it indicates that the Ce 3d_{5/2} signals consist of a photoelectron peak 882.1 eV for $\text{Ce}_6\text{MoO}_{15-\delta}$. The curve (b) is the standard photoelectron peak of CeO_2 , which the valence state of Ce is 4+ valences in CeO_2 [12,13]. It indicates that the valence state of Ce in new compound also is 4+ valences. The photoelectron peaks of the Mo 3d in $\text{Ce}_6\text{MoO}_{15-\delta}$ are also given in Fig. 2. Through the binding energy of Mo 3d_{5/2} (231.9 eV), it indicates that the peaks could be assigned to Mo^{6+} species. It is admirably coincide with the data reported in the literatures [14,15]. This indicates that the Ce and Mo ions are 4+ and 6+ valence, respectively, in the new compound. According to the principle of the charge balance, the defined chemical formula of new compound will be $\text{Ce}_6\text{MoO}_{15-\delta}$.

In order to further prove the valence of Ce ion in new compound, the Raman spectrum of CeO_2 , $\text{Ce}_6\text{MoO}_{15-\delta}$ and

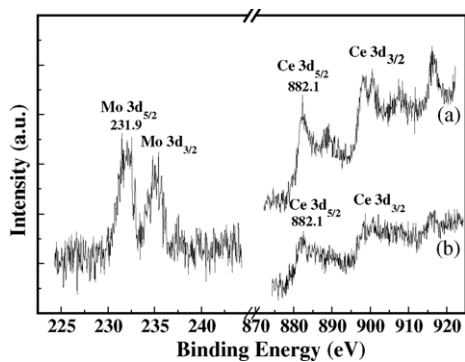
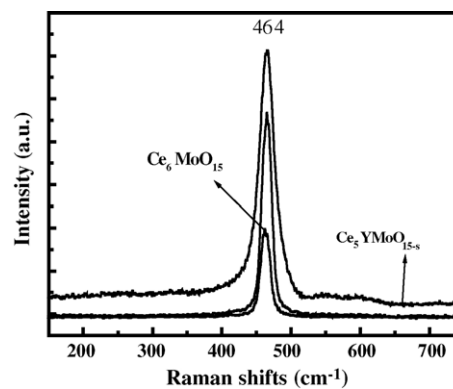
Fig. 2. XPS of (a) CeO_2 and (b) $\text{Ce}_6\text{MoO}_{15-\delta}$.

Fig. 3. Raman spectrum of samples.

$\text{Ce}_5\text{YMoO}_{15-\delta}$ is shown in Fig. 3. From Fig. 3, the Raman peak of CeO_2 is lied at about 464 cm^{-1} , which is the character Raman peak of Ce^{4+} with the Raman-active F_{2g} mode of fluorite-related dioxides [11]. Also, it is very obvious that the Raman peak of $\text{Ce}_6\text{MoO}_{15-\delta}$ and $\text{Ce}_5\text{YMoO}_{15-\delta}$ is all have a similar Raman spectrum with CeO_2 at 464 cm^{-1} .

By comparison with the spectrum of CeO_2 , also shown in Fig. 3, it is evident that the sample $\text{Ce}_6\text{MoO}_{15-\delta}$ shows no other peaks besides F_{2g} band. It proved that the two compounds have the same symmetry. For $\text{Ce}_5\text{YMoO}_{15-\delta}$, the F_{2g} mode becomes asymmetric with a broad tail in the range $525\text{--}625 \text{ cm}^{-1}$ which was assigned to a contribution of the oxygen vacancies [16]. The 464 cm^{-1} peak can be considered as a symmetric breathing mode of the oxygen atoms around Ce^{4+} and Mo^{6+} . This also prove the valence in $\text{Ce}_{6-x}\text{Ln}_x\text{MoO}_{15-\delta}$ is 4+ for Ce ion and 6+ for Mo ion, respectively.

Typical A.C. impedance spectra of $\text{Ce}_5\text{YMoO}_{15-\delta}$ and $\text{Ce}_{5/6}\text{Y}_{1/6}\text{O}_{2-\delta}$ with two impedance semi-circles are shown in Fig. 4. It is the typical impedance spectrum of ionic conductor. It is seen in Fig. 4, the impedance spectra of the two samples are very similar at 350°C , and they all could be resolved into a bulk, grain boundary, and electrode polarization semi-circle at high, middle and low frequencies, respectively. Their resistivity is very high. But at 650°C , the grain boundary semi-circle can be ignored, their resistivity become smaller than that at 350°C , as shown in Fig. 4. It is known that if the system is pure electron conductivity, the curve will be a straight line with perpendicular to the real axis [17]. From the Fig. 4, it is obvious that two typical A.C. impedance semi-circles indicate the ionic conductivity for the new compound.

Since it was considered that the impedance semi-circle was related to the ionic conduction in the bulk and the grain boundary, the resistance of the samples was determined from the interceptions of the high frequency arc on the real axis. Therefore, it is easy to separate the resistance of bulk (R_{bulk}) and that of grain boundary (R_{gb}) from impedance spectroscopy measured. The total resistance was converted to the electrical conductivity by consideration of the thickness and area of the sample. The impedance spec-

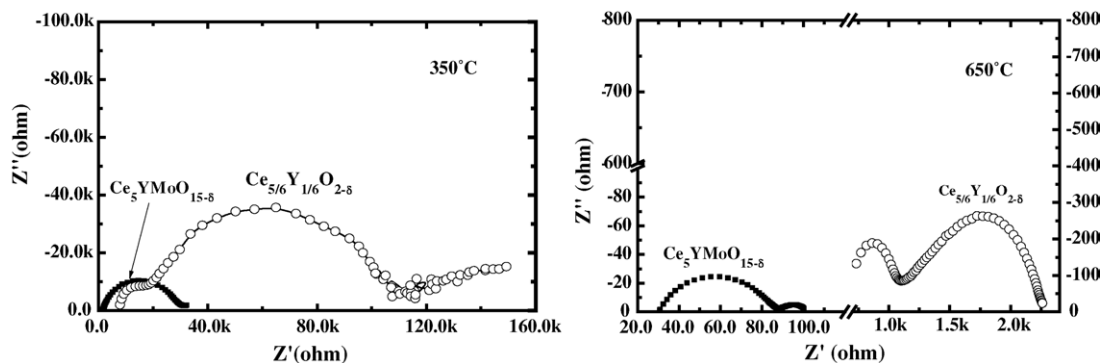


Fig. 4. Impedance spectra of $\text{Ce}_{5/6}\text{Y}_{1/5}\text{O}_{2-\delta}$ and $\text{Ce}_5\text{YMoO}_{15-\delta}$.

troscopy measurement shows that at same temperature, the resistance of compound $\text{Ce}_{5/6}\text{Y}_{1/5}\text{O}_{2-\delta}$ is higher than that of $\text{Ce}_5\text{YMoO}_{15-\delta}$. Especially, at 650°C the resistivity of $\text{Ce}_5\text{YMoO}_{15-\delta}$ is about two order of magnitude smaller than that of $\text{Ce}_{5/6}\text{Y}_{1/5}\text{O}_{2-\delta}$. It indicates that $\text{Ce}_5\text{YMoO}_{15-\delta}$ is a good oxide ionic conductor compared with $\text{Ce}_{5/6}\text{Y}_{1/5}\text{O}_{2-\delta}$ in the intermediate temperature range.

The temperature dependence of the conductivity for $\text{Ce}_6\text{MoO}_{15-\delta}$, $\text{Ce}_{5/6}\text{Y}_{1/5}\text{O}_{2-\delta}$ and $\text{Ce}_5\text{LnMoO}_{15-\delta}$ ($\text{Ln} = \text{Y}, \text{Pr}, \text{Sm}, \text{Tb}, \text{Dy}, \text{Ho}, \text{Er}$ and Yb) was given in Fig. 5.

With increasing temperature, the conductivity of all the samples increases linearly without any abrupt conductivity change in the Arrhenius plots of the conductivity. The oxide ionic conductivity in $\text{Ce}_6\text{MoO}_{15-\delta}$ is nearly two order of magnitude higher than that of $\text{Ce}_{5/6}\text{Y}_{1/5}\text{O}_{2-\delta}$ above 550°C . This increase of ionic conductivity is attributed to the association of defects. The oxide ionic conductivity is the product of the intrinsic oxygen vacancies and ionic mobility [18]. At high temperature, many oxygen vacancies are free and mobile, which leads to a sharp increase in oxide ionic conductivity. On the other hand, at relatively low temperatures, all the vacancies are trapped and the concentration of free vacancies, then, decreases with decreasing temperature. It results to low oxide conductivity. The character vacancies in the compounds $\text{Ce}_5\text{LnMoO}_{15-\delta}$ ($\text{Ln} = \text{Y}, \text{Pr}, \text{Sm}, \text{Tb}, \text{Dy}, \text{Ho}, \text{Er}$ and Yb) result from substitution of the rare earths for Ce.

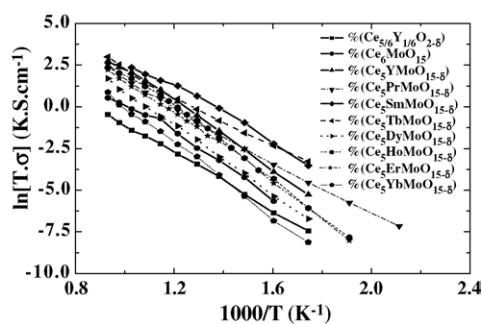


Fig. 5. Conductivity vs. temperature for $\text{Ce}_6\text{MoO}_{15-\delta}$, $\text{Ce}_{5/6}\text{Y}_{1/5}\text{O}_{2-\delta}$ and $\text{Ce}_5\text{LnMoO}_{15-\delta}$ ($\text{Ln} = \text{Y}, \text{Pr}, \text{Sm}, \text{Tb}, \text{Dy}, \text{Ho}, \text{Er}$ and Yb).

4. Conclusions

We have successfully synthesized a new compound $\text{Ce}_6\text{MoO}_{15-\delta}$. Structural characterization shows that new compound $\text{Ce}_6\text{MoO}_{15-\delta}$ and its Ln-doped samples $\text{Ce}_5\text{LnMoO}_{15-\delta}$ have cubic fluorite structure with space group $Fm\bar{3}m$. And all the synthesized molybdates remain MoO_6 octahedra. The variation of the lattice parameters is well in agreement with decrease of the ionic radius of rare earths. Enhanced conductivity of $\text{Ce}_5\text{LnMoO}_{15-\delta}$ ($\text{Ln} = \text{Y}, \text{Pr}, \text{Sm}, \text{Gd}, \text{Tb}, \text{Dy}, \text{Ho}, \text{Er}$ and Yb) originates from the oxygen vacancies. New compound $\text{Ce}_5\text{LnMoO}_{15-\delta}$ have higher oxide ionic conductivity compared with $\text{Ce}_{5/6}\text{Y}_{1/5}\text{O}_{2-\delta}$ above 650°C , $\text{Ce}_5\text{LnMoO}_{15-\delta}$ have two order of magnitude higher than that of $\text{Ce}_{5/6}\text{Y}_{1/5}\text{O}_{2-\delta}$ in conductivity and shows a potential application in the intermediate temperature range for SOFCs.

Acknowledgment

This work was supported by National Natural Science Foundation of China (20271049, 20331030).

References

- [1] V. Vladislav, N. Kharton Evgeny, A.N. Alim, M. Vecher, J. Solid State Electrochem. 3 (1999) 61.
- [2] V. Vladislav, N.K. Kharton Evgeny, A. Naumovich, et al., J. Solid State Electrochem. 5 (2001) 160.
- [3] H. Inaba, H. Tagawa, Solid State Ionics 83 (1996) 1.
- [4] T. Ishihara, H. Matsuda, Y. Takita, J. Am. Chem. Soc. 116 (1994) 3801.
- [5] T. Ishihara, Y. Hiei, Y. Takita, Solid State Ionics 79 (1995) 371.
- [6] T. Ishihara, H. Furutani, Chem. Mater. 11 (1999) 2081.
- [7] P. Lacorre, F. Goutenoire, O. Bolmke, R. Retoux, Y. Laligant, Nature 404 (2000) 856.
- [8] T. Ishihara, H. Arikawa, T. Akbay, H. Nishiguchi, Y. Takita, J. Am. Chem. Soc. 123 (2001) 203.
- [9] C. Marcilly, P. Courty, B. Delmon, J. Am. Ceram. Soc. 53 (1970) 56.
- [10] Y. Takaki, T. Taniguchi, K. Hori, J. Ceram. Soc. Jpn. 101 (1993) 373.

- [11] J.R. McBride, K.C. Hass, B.D. Poindexte, W.H. Weber, *J. Appl. Phys.* 76 (1994) 2435.
- [12] V.I. Nefedov, D. Gati, B.F. Dzhurinskii, N.P. Sergushin, Y.V. Salyn, *Zh. Neorg. Khim.* 20 (1975) 2307.
- [13] C.H. Steele Brian, Heinzl Angelika, *Nature* 414 (2001) 345–352.
- [14] A. Cimino, B.A. De Angelis, *J. Catal.* 136 (1975) 11.
- [15] C.V. Caceres, J.L.G. Fierro, J. Lazaro, A.L. Agudo, J. Soria, *J. Catal.* 122 (1990) 113.
- [16] A. Mineshige, T. Taji, M. Kobune, S. Fujii, et al., *Solid State Ionics* 135 (2000) 481.
- [17] P. Hagenmuller, W. Van Gool, *Solid Electrolytes*, Academic Press, New York, 1978.
- [18] T. Norby, *J. Mater. Chem.* 11 (2001) 11.